Structural Engineering and Mechanics, Vol. 21, No. 2 (2005) 205-220
DOI: http://dx.doi.org/10.12989/sem.2005.21.2.205

Application of artificial neural networks to a double receding contact problem with a rigid stamp

Erdoğan Çakıroğlu†, İsa Çömez‡ and Ragıp Erdöl‡†

Karadeniz Technical University, Civil Engineering Department, 61080, Trabzon, Turkey

(Received December 7, 2004, Accepted July 6, 2005)

Abstract. This paper presents the possibilities of adapting artificial neural networks (ANNs) to predict the dimensionless parameters related to the maximum contact pressures of an elasticity problem. The plane symmetric double receding contact problem for a rigid stamp and two elastic strips having different elastic constants and heights is considered. The external load is applied to the upper elastic strip by means of a rigid stamp and the lower elastic strip is bonded to a rigid support. The problem is solved under the assumptions that the contact between two elastic strips also between the rigid stamp and the upper elastic strip are frictionless, the effect of gravity force is neglected and only compressive normal tractions can be transmitted through the interfaces. A three layered ANN with backpropagation (BP) algorithm is utilized for prediction of the dimensionless parameters related to the maximum contact pressures. Training and testing patterns are formed by using the theory of elasticity with integral transformation technique. ANN predictions and theoretical solutions are compared and seen that ANN predictions are quite close to the theoretical solutions. It is demonstrated that ANNs is a suitable numerical tool and if properly used, can reduce time consumed.

Key words: contact problem; contact pressure; contact length; elasticity; rigid stamp; backpropagation; artificial neural networks.

1. Introduction

The human brain is a very powerful instrument for all kinds of tasks, from vision and hearing to steering the muscles. Probably the most interesting feature is its capability to learn and to anticipate new tasks. This capacity of the brain has inspired many scientists to model artificial intelligence (AI) techniques. There are different types of AI techniques and ANNs is one of the widely used AI techniques to solve engineering problems.

By the improvement of the computer technology, computers become an integral part of day to day activities and engineers have utilized various applications with ANN. Several authors have used ANNs in engineering applications and many reliable results have been produced.

Vanluchene and Sun (1990) have demonstrated the potential of the ANNs approach to three structural engineering applications. The first problem involves a simple beam load location; the

† Research Assistant, Corresponding author, E-mail: erdoganc@ktu.edu.tr
‡ Research Assistant
‡† Professor

second problem is a simple concrete beam design; and the third problem is a simple supported rectangular plate analysis. The behaviors of the concrete in the state of plane stress under monotonic biaxial loading and compressive uniaxial cycle loading are modeled with ANNs by Ghaboussi *et al.* (1991). The role of neural computing on the structural analysis and design is examined by Hajela and Berke (1991). They have represented the force-displacement relationship in static structural analysis with ANNs which can be used for rapid analysis for structural optimization. The effect of representation on the performance of ANNs in structural engineering applications is studied by Gunaratnam and Gero (1994). They have suggested that dimensional analysis provides a suitable representation framework for training the input-output patterns. ANN which replaces to an anisotropic hardening plasticity problem through an appropriate sequence of anisotropic elasticity problems is illustrated by Theocaris and Panagiotopoulos (1995). ANN approach for the detection of the changes in the characteristics of the structure systems is presented by Masri *et al.* (1996). The size effects in fracture of cementitious materials with ANN model built from experimental data is examined by Arslan and Ince (1996). The potential use of ANNs in the field of fracture mechanics is explored by Seibi and Alawi (1997). They have predicted the fracture toughness of an aluminum alloy based on experimental data, and explored the effect of crack geometry, temperature and biaxiality on fracture toughness. The estimation of the contact force on laminated composite plates subjected to low velocity impact with ANN is considered by Chandrashekhara *et al.* (1998). They have formed the training set by using the contact force and strain histories obtained from finite element simulation results. The load deflection behavior of concrete slabs, the final crack-pattern formation of concrete slabs, and both the concrete and reinforcing-steel strain distribution at failure prediction with ANN approach is examined by Hegazy *et al.* (1998). The prediction of 28-day compressive strength of concrete by using ANNs based on the inadequacy of present methods dealing with multiple variable and nonlinear problems is considered by Ni and Wang (2000). The use of ANNs in predicting the ultimate shear strength of reinforced concrete deep beams is explored by Sanad and Saka (2001). They have collected one hundred eleven experimental data from literature covering the case of simply supported beams with two point loads acting symmetrically with respect to the centerline of the span. The detection and classification of flaws in concrete structure is studied by Xiang and Tso (2002). They have concerned with the feature extraction from bispectra for concrete flaw detection. Impact-echo experiments are carried out for three different types of flaw in concrete structure and features are selected from the modules of bispectra in the primary region and ANN is used as a classifier. The potential use of ANNs in the field of contact mechanics is examined by Ozsahin *et al.* (2004). They have developed ANN model for predicting the contact lengths between the elastic layer and two elastic circular punches.

In this study, an ANN approach is utilized to predict the dimensionless parameters related to the maximum contact pressures of the plane symmetric double receding contact problem of a rigid stamp and two elastic strips with different elastic constants and heights. Analytic solution of the problem is obtained by Comez *et al.* (2004). The input and output values of the training and testing set patterns are formed using the theoretical solution. The best generalization and the minimum ANN structure are determined by trial and error. After training, ANN test predictions and the effect of some factors on the dimensionless parameters related to the maximum contact pressures are compared with theoretical solutions.

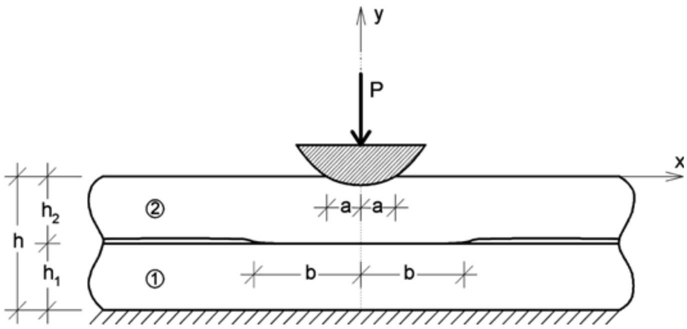

Fig. 1 Geometry of the contact problem

2. Theoretical solution of the contact problem

The plane symmetric double receding contact problem for a rigid stamp and two elastic strips with different elastic constants and heights is shown in Fig. 1. The external load is applied to the upper elastic strip by means of a rigid stamp and the lower elastic strip is bonded to a rigid support. The problem is solved under the assumptions that the contact between two elastic strips also between the rigid stamp and the upper elastic strip are frictionless, the effect of gravity force is neglected and only compressive normal tractions can be transmitted through the interfaces.

The analytical solution of the problem studied by Comez *et al*. (2004) is summarized in the following:

Observing that the system is symmetrical about y axis at $x = 0$, it is sufficient to consider the problem only in the region $0 \le x < \infty$. Using the symmetry and Fourier transform technique, the following expressions may be written

$$u_i(x, y) = \frac{2}{\pi}\int_0^\infty \Phi_i(\alpha, y)\sin(\alpha x)d\alpha \tag{1a}$$

$$v_i(x, y) = \frac{2}{\pi}\int_0^\infty \Psi_i(\alpha, y)\cos(\alpha x)d\alpha \qquad (i = 1, 2) \tag{1b}$$

where u and v are the x and y - components of the displacement vector. Φ_i and Ψ_i $(i = 1, 2)$ functions are inverse Fourier transforms of u_i and v_i, respectively. Taking necessary derivatives of Eqs. (1a) and (1b), and substituting them into Navier equations, and solving second order differential equations, the following expressions may be obtained for displacements:

$$u_i(x, y) = \frac{2}{\pi}\int_0^\infty [(A_i + B_i y)e^{-\alpha y} + (C_i + D_i y)e^{\alpha y}]\sin(\alpha x)d\alpha \tag{2a}$$

$$v_i(x, y) = \frac{2}{\pi}\int_0^\infty \left\{\left[A_i + \left(\frac{\kappa_i}{\alpha} + y\right)B_i\right]e^{-\alpha y} + \left[-C_i + \left(\frac{\kappa_i}{\alpha} - y\right)D_i\right]e^{\alpha y}\right\}\cos(\alpha x)d\alpha \tag{2b}$$

where A_i, B_i, C_i and $D_i (i = 1, 2)$ are the unknown functions which will be determined from the boundary conditions prescribed on $y = 0$, $y = -h_2$ and $y = -h$ of the problem. $\kappa_i = (3 - \nu_i)/(1 + \nu_i)$ for plane stress and $\kappa_i = 3 - 4\nu_i$ for plane strain, ν_i being the Poisson's ratio. Using Hooke's law and Eqs. (2a) and (2b), the stress components may be expressed as follows:

$$\frac{1}{2\mu_i}\sigma_{xi}(x,y) = \frac{2}{\pi}\int_0^\infty \left\{ \left[\alpha(A_i + B_i y) - \frac{3-\kappa_i}{2}B_i\right]e^{-\alpha y} + \left[\alpha(C_i + D_i y) + \frac{3-\kappa_i}{2}D_i\right]e^{\alpha y} \right\}\cos(\alpha x)\,d\alpha \tag{3a}$$

$$\frac{1}{2\mu_i}\sigma_{yi}(x,y) = \frac{2}{\pi}\int_0^\infty \left\{ -\left[\alpha(A_i + B_i y) + \frac{1+\kappa_i}{2}B_i\right]e^{-\alpha y} + \left[-\alpha(C_i + D_i y) + \frac{1+\kappa_i}{2}D_i\right]e^{\alpha y} \right\}\cos(\alpha x)\,d\alpha \tag{3b}$$

$$\frac{1}{2\mu_i}\tau_{xyi}(x,y) = \frac{2}{\pi}\int_0^\infty \left\{ -\left[\alpha(A_i + B_i y) + \frac{\kappa_i-1}{2}B_i\right]e^{-\alpha y} + \left[\alpha(C_i + D_i y) - \frac{\kappa_i-1}{2}D_i\right]e^{\alpha y} \right\}\sin(\alpha x)\,d\alpha \tag{3c}$$

The plane double receding contact problem outlined above as shown in Fig. 1 must be solved under the following boundary conditions:

$$\sigma_{y2}(x,0) = \begin{cases} -p_2(x) & 0 \le x < a \\ 0 & a \le x < \infty \end{cases} \tag{4a}$$

$$\tau_{xy2}(x,0) = 0 \qquad (0 \le x < \infty) \tag{4b}$$

$$\sigma_{y1}(x,-h_2) = \begin{cases} -p_1(x) & 0 \le x < b \\ 0 & b \le x < \infty \end{cases} \tag{4c}$$

$$\tau_{xy2}(x,-h_2) = 0 \qquad (0 \le x < \infty) \tag{4d}$$

$$\tau_{xy1}(x,-h_2) = 0 \qquad (0 \le x < \infty) \tag{4e}$$

$$\sigma_{y1}(x,-h_2) = \sigma_{y2}(x,-h_2) \qquad (0 \le x < \infty) \tag{4f}$$

$$v_1(x,-h) = 0 \qquad (0 \le x < \infty) \tag{4g}$$

$$u_1(x,-h) = 0 \qquad (0 \le x < \infty) \tag{4h}$$

$$\frac{\partial v_2(x,0)}{\partial x} = \frac{\partial F(x)}{\partial x} \qquad (0 \le x < a) \tag{4i}$$

$$\frac{\partial v_1(x,-h_2)}{\partial x} = \frac{\partial v_2(x,-h_2)}{\partial x} \qquad (0 \le x < b) \tag{4j}$$

where a is the half-width of the contact length between the rigid stamp and the upper elastic strip, b is the half-width of the contact length between the two elastic strips, $F(x)$ is a known function obtained the equation giving the profile of the rigid stamp, $p_2(x)$ and $p_1(x)$ are the unknown contact pressures on the contact lengths a and b, respectively.

By making use of the boundary conditions (4a-h), eight of the unknown constants A_i, B_i, C_i and $D_i (i = 1, 2)$ appearing in Eqs. (2) and (3) may be obtained in terms of the unknown functions $p_2(x)$ and $p_1(x)$. Thus, the stresses and the displacements can be expressed depending on the unknown contact pressures $p_2(x)$ and $p_1(x)$.

The new unknown functions $p_2(x)$ and $p_1(x)$ are determined from the conditions (4i) and (4j) which have not yet been satisfied. These conditions give the following system of integral equations, after some routine manipulations and using the symmetry:

$$\frac{1}{\pi}\int_{-a}^{a}\left[\frac{1}{t-x} + k_1(x,t)\right]p_2(t)dt + \frac{1}{\pi}\int_{-b}^{b}k_2(x,t)p_1(t)dt = l(x) \qquad (-a < x < a) \tag{5a}$$

$$\frac{1}{\pi}\int_{-b}^{b}\left[\frac{1}{t-x} + k_3(x,t)\right]p_1(t)dt + \frac{1}{\pi}\int_{-a}^{a}k_4(x,t)p_2(t)dt = 0 \qquad (-b < x < b) \tag{5b}$$

where $k_1(x,t)$, $k_2(x,t)$, $k_3(x,t)$, $k_4(x,t)$ and $l(x)$ are defined in Comez *et al.* (2004).

In the system of singular integral Eqs. (5a) and (5b) in addition to the contact pressures (stresses) $p_2(x)$ and $p_1(x)$, the half-width of the contact lengths a and b are also unknown. These two unknowns a and b are determined from the equilibrium conditions which may be expressed as

$$\int_{-a}^{a} p_2(t)dt = P \tag{6a}$$

$$\int_{-b}^{b} p_1(t)dt = P \tag{6b}$$

where P is the known (compressive) resultant force applied to the rigid stamp away from the contact region ($y = 0,\ -a < x < a$).

Designating the variables (x, t) on $y = -h_2$ and $y = 0$ by (x_1, t_1) and (x_2, t_2) respectively, and defining the following dimensionless quantities;

$$r_1 = x_1/b, \qquad r_2 = x_2/a \tag{7a}$$

$$s_1 = t_1/b, \qquad s_2 = t_2/a \tag{7b}$$

$$g_1(s_1) = \frac{p_1(t_1)}{P/h_2} \qquad g_2(s_2) = \frac{p_2(t_2)}{P/h_2} \tag{7c}$$

$$\eta = \frac{\mu_2}{P/h_2} \tag{7d}$$

where μ_2 is the upper elastic strip shear modulus. The system of integral Eqs. (5a) and (5b) may be expressed as follows:

$$\frac{1}{\pi}\int_{-1}^{1}\left[\frac{1}{s-r}+\frac{a}{h_2}m_1(r,s)\right]g_2(s)ds+\frac{1}{\pi}\frac{b}{h_2}\int_{-1}^{1}m_2(r,s)g_1(s)ds = l^*(r) \qquad (-1<r<1) \tag{8a}$$

$$\frac{1}{\pi}\int_{-1}^{1}\left[\frac{1}{s-r}+\frac{b}{h_2}m_3(r,s)\right]g_1(s)ds+\frac{1}{\pi}\frac{b}{h_2}\int_{-1}^{1}m_4(r,s)g_2(s)ds = 0 \qquad (-1<r<1) \tag{8b}$$

where $m_1(r,s)$, $m_2(r,s)$, $m_3(r,s)$, $m_4(r,s)$ and $l^*(r)$ are defined in Comez *et al.* (2004).

Similarly, the additional conditions (6a) and (6b) may be expressed as

$$\frac{a}{h_2}\int_{-1}^{1}g_2(s)ds = 1 \tag{9a}$$

$$\frac{b}{h_2}\int_{-1}^{1}g_1(s)ds = 1 \tag{9b}$$

In order to solve the system of integral equations, it is found that the integral Eqs. (8a) and (8b) has an index −1 (Erdogan and Gupta 1972) because of the smooth contact at the end points a and b. To insure smooth contact at the end points a and b, let

$$g_1(s) = G_1(s)(1-s^2)^{1/2} \qquad (-1<s<1) \tag{10a}$$

$$g_2(s) = G_2(s)(1-s^2)^{1/2} \qquad (-1<s<1) \tag{10b}$$

where $G_1(s)$ and $G_2(s)$ are bounded functions. Using the Gauss-Chebyshev integration formulas (Erdogan and Gupta 1972), Eqs. (8a), (8b), (9a) and (9b) become

$$\sum_{k=1}^{N}\frac{(1-s_k^2)}{N+1}\left\{\left[\frac{1}{s_k-r_i}+\frac{a}{h_2}m_1(r_i,s_k)\right]G_2(s_k)+\frac{b}{h_2}m_2(r_i,s_k)G_1(s_k)\right\} = \frac{1}{\pi}l^*(r_i)$$

$$(i = 1, \ldots, N+1) \tag{11a}$$

$$\sum_{k=1}^{N}\frac{(1-s_k^2)}{N+1}\left\{\left[\frac{1}{s_k-r_i}+\frac{b}{h_2}m_3(r_i,s_k)\right]G_1(s_k)+\frac{b}{h_2}m_4(r_i,s_k)G_2(s_k)\right\} = 0$$

$$(i = 1, \ldots, N+1) \tag{11b}$$

$$\frac{a}{h_2}\sum_{k=1}^{N}\frac{(1-s_k^2)}{N+1}G_2(s_k) = \frac{1}{\pi} \tag{11c}$$

$$\frac{b}{h_2}\sum_{k=1}^{N}\frac{(1-s_k^2)}{N+1}G_1(s_k) = \frac{1}{\pi} \tag{11d}$$

where,

$$s_k = \cos\left(\frac{k\pi}{N+1}\right) \qquad (k = 1, \ldots, N) \tag{12a}$$

$$r_i = \cos\left(\frac{\pi}{2}\frac{2i-1}{N+1}\right) \qquad (i = 1, \ldots, N+1) \tag{12b}$$

The Eqs. (11a), (11b), (11c) and (11d) give $2N+2$ algebraic equations to determine the $2N+2$ unknowns $G_1(s_k)$, $G_2(s_k)$, ($k=1$, ..., N), a and b. The system of equations are linear in $G_1(s_k)$ and $G_2(s_k)$, but highly nonlinear in a and b. Therefore, a time consuming interpolation and iteration scheme had to be used to obtain these two unknowns.

It is seen from contact pressure distribution that the maximum contact pressures between the rigid stamp and the upper elastic strip, and between the two elastic strips take place at $x = 0$.

3. Application of the artificial neural network approach to the contact problem

Basically, ANNs simulate the biological neural system and intend to imitate the behavior of biological learning and decision making. In the ANN, the basic unit is called artificial neuron or processing element (PE). ANNs are computing systems made up of a simple and highly interconnected PEs that process information by their dynamic state response to external inputs. Every PE may have several input paths. The PE combines, usually by a simple summation, the weighted values of these input paths. The result is internal activity level for the PE. The combined values are then modified by an activation function.

In ANNs, learning is to modify the variable connection weights on the inputs of each PE in order to achieve the desired results for a given set of inputs. There are two types of learning; supervised and unsupervised. In supervised learning, the ANN output(s) is compared to the desired output(s). Weights are then adjusted by the network so that the next iteration can produce a closer match between desired and ANNs output(s). The global error reduction is created over time by continuously by modifying the initial weights until acceptable error is reached.

Many researchers have developed various ANN models for different purposes. The most popular supervised learning approach is multi layer perceptron (MLP) architecture. The MLP learns via backpropagation (BP) algorithm, which uses the gradient-descent method to minimize the error function (Rumelhart 1986). This algorithm necessitates the use of a continuous differentiable weighting function; therefore, sigmoid activation function has been used in most ANNs. The learning rule associated with BP is known as the generalized delta rule. Fig. 2 shows a processing element and the sigmoid activation function.

Where $x_i(i = 1, \ldots, m)$ is the inputs, $w_{ij}(j = 1, \ldots, n)$ is the weights of the inputs, net_j is weighted summation and y is the sigmoid activation function in the range of $[0-1]$.

Basically, all ANNs have a similar structure of topology. PEs are usually organized into groups called layers. The layers are called input layer, hidden layer(s) (one or more, especially one) and

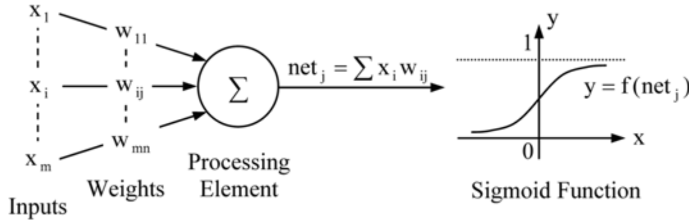

Fig. 2 A processing element and sigmoid function

output layer. Each PE is independent in its layer, but is connected to all of the PEs in the next layer with weights. The number of PEs in the input and output layers are determined by the design requirements. However, there is no general rule for selecting the number of PEs in the hidden layer and the number of PEs in the hidden layer seriously affects the outcome of the network training. It is mainly problem specific but it should be sufficiently low and ensure generalization. If too few PEs are included, the network may not be able to learn properly and the predictions of the network to testing patterns will be poor. On the other hand, if too many PEs are included, the network becomes over trained and may provide erroneous predictions to testing patterns. The best structure of the ANN requires trial and error. A general MLP architecture, a three layered ANN with a BP algorithm, is shown in Fig. 3.

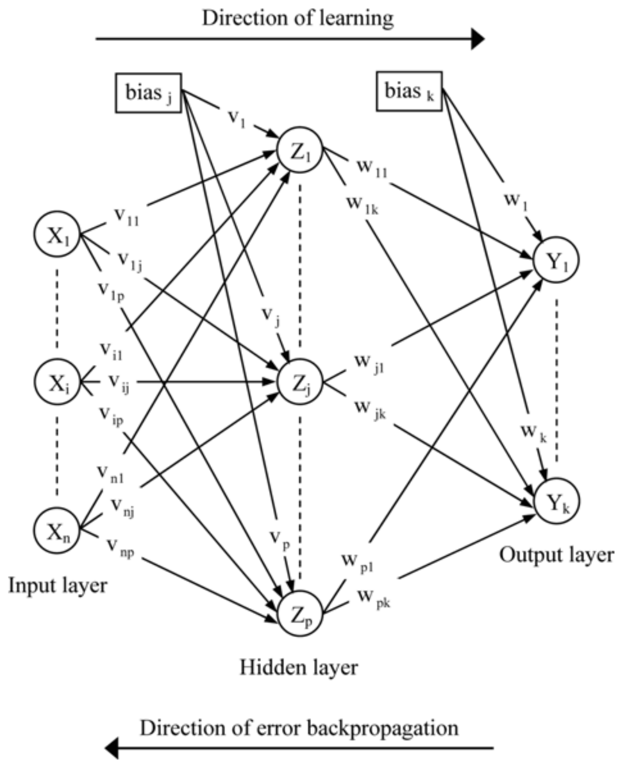

Fig. 3 The ANN architecture with BP algorithm

Where $X_i(i = 1, \ldots, n)$, $Z_j(j = 1, \ldots, p)$ and $Y_k(k = 1, \ldots, m)$ are input, hidden and output layer PEs; v_{ij} and w_{jk} are the weights from input to hidden layer, and hidden to output layer; v_j and w_k are the biases of hidden and output layer, respectively.

Training a network by BP algorithm involves three stages; feedforward of training set, backpropagation of associated error and adjustments of weights and biases. The procedures of the ANNs are widely given in Zurada (1992) and Fausett (1994).

If the ANN is trained well, it can quickly predict the corresponding output(s) for any given inputs. It predicts the output(s) of the testing pattern using the existing weight values developed in the training. The predictions are extremely rapid because the network only calculates the input and weight values once. This feature provides time gaining especially in time consuming problems.

As it is stated before, the aim of this paper is to investigate the performance of ANNs in predicting dimensionless parameters related to the maximum contact pressures by using the BP algorithm. There are many ANN programs available. In this study, a program written in C++ has been utilized for predicting the dimensionless parameters related to the maximum contact pressures.

A three layered ANN structure is selected like in Fig. 3. In this study, different combination of the force, geometry and material properties have been formed for the input layer. These are 6 PEs corresponding to the 6 dimensionless variables. These dimensionless variables are:

η : Dimensionless quantity given in Eq. (7d)
R/h_2 : Ratio of radius of rigid stamp to upper elastic strip height
h_2/h_1 : Ratio of upper and lower elastic strip heights
μ_2/μ_1 : Ratio of upper and lower elastic strip shear modulus
κ_2 : Elastic constant of the upper strip
κ_1 : Elastic constant of the lower strip

and there are 2 PEs in the output layer corresponding to the 2 dimensionless parameters related to the maximum contact pressures. These are:

$p_2^{\max} \cdot h_2/P$: Dimensionless parameter related to the maximum contact pressure between the rigid stamp and the upper elastic strip
$p_1^{\max} \cdot h_2/P$: Dimensionless parameter related to the maximum contact pressure between the two elastic strips.

The values of the input variables used for training set are presented in Table 1.

225 patterns which are different combinations of the values in Table 1 are solved theoretically to form the training set. In addition, 45 patterns apart from the values in Table 1 are solved to form the testing set.

Table 1 Input values used for training set

η	R/h_2	h_2/h_1	μ_2/μ_1	κ_2	κ_1
		0.25	0.0625		
250	125	0.5	0.25	1.8	1.8
500	250	1	1	2	2
1000	500	2	4	2.2	2.2
		4	16		

Because of the feature of the sigmoid function, pattern's input-output values obtained from theoretical solution need to be normalized into the range of $[0-1]$. Besides, selecting the normalization ranges, such as $[0.1-0.9]$, instead of the boundary range $[0-1]$ greatly decreases the training time. Normalization can be linear or nonlinear depending on the distribution of the training and testing sets. In this problem, each column of the pattern input-output values is normalized into different ranges. As seen in Table 1, each column's minimum and maximum values are in different ranges, so that, each input and output columns are normalized with different functions and different ranges. First four input columns are normalized into different logarithmic functions scaled in the ranges of $[0.30-0.70]$, $[0.34-0.66]$, $[0.40-0.60]$ and $[0.38-0.62]$, respectively. The last two input columns are normalized into linear function scaled in the range of $[0.49-0.51]$. Similarly, the output columns are normalized into different nonlinear functions in the ranges of $[0.20-0.80]$ and $[0.30-0.70]$, respectively.

The number of PEs in the hidden layer of the network is a harmony between convergence and generalization. Convergence is the capacity of the network to learn the pattern on the training set and generalization is the capacity to predict on the testing patterns.

The most important factor for the convergence is the initial weight values. They affect the reaching of a global minimum error. The update of weight values depends on the derivative of the former activation function and the latter activation function. Therefore, it is important to avoid choices of initial values that would make it likely that either activation functions or derivatives of activation functions are zero. In addition, α, the learning rate, also affects the convergence. α is the constant proportionality of the generalization. The more learning rate the more changes in weights.

4. Results and discussion

Many network structures have been tried by trial and error. It is found that, there is a trade off between the capacity of a network and time consumed. Usually, the capacity of a network is found to increase with suitable increase in the training set patterns and the number of PEs in the hidden layer. In the meantime, the increase of these also increases training time.

The relative error is computed as $e_{rel} = \left|\frac{O_{actual} - O_{ANN}}{O_{actual}}\right| * 100$, where O_{actual} and O_{ANN} are the theoretical solution and ANN prediction of the $p_2^{\max} \cdot h_2/P$ and $p_1^{\max} \cdot h_2/P$. Training is stopped when each output relative error in normalized training set is less than 1.50%. The aim is to determine the best generalization and the minimum number of PEs in the hidden layer. Because of this, different hidden layer PEs, learning rate and initial weight values are tried by trial and error to determine the appropriate network structure. As a result, the network structure of the 6-18-2 with $\alpha = 0.5$ and the initial weights chosen random in the range of $[0.05-0.30]$ gives the best generalization. Training time is approximately 10 hr on a personal computer and predicts testing patterns in 1 second on the same PC. Different network structures with different learning rate and initial weight values may produce better convergence and generalization and smaller relative error.

The testing set is used to evaluate the capacity of the trained ANN structure. 45 testing set patterns input values and desired outputs are presented in Table 2. The maximum relative errors of the $p_2^{\max} \cdot h_2/P$ and $p_1^{\max} \cdot h_2/P$ in the testing set are calculated as 2.77% and 1.81%, respectively and Fig. 4 is an expression of the learning capacity of the network on the $p_2^{\max} \cdot h_2/P$ and

Table 2 Testing set patterns

No	Input values						Desired outputs	
	η	R/h_2	h_2/h_1	μ_2/μ_1	κ_2	κ_1	$p_2^{max} \cdot h_2/P$	$p_1^{max} \cdot h_2/P$
1	300	180	0.40	12.50	2.18	1.85	0.97862	0.49112
2	675	135	0.60	14.00	2.16	1.81	1.84353	0.46607
3	450	200	1.60	1.60	2.10	2.05	1.28290	0.60791
4	470	170	2.50	0.07	1.81	2.16	1.62501	0.84580
5	625	175	0.15	2.85	2.12	2.01	1.71651	0.77030
6	550	550	0.45	0.80	2.02	2.06	0.95200	0.68527
7	950	475	0.55	1.25	1.92	1.88	1.31641	0.70670
8	780	190	1.20	0.09	1.79	2.15	1.96951	0.86682
9	700	170	0.75	1.90	2.13	2.06	1.78842	0.66422
10	270	215	2.75	10.50	2.16	1.85	0.54971	0.32833
11	610	290	2.50	0.12	1.84	2.11	1.41467	0.80882
12	300	150	3.00	2.75	2.17	2.08	1.09439	0.50971
13	475	175	0.40	0.10	1.82	2.13	1.61259	0.85459
14	275	275	0.20	0.20	1.95	2.14	1.00413	0.75261
15	650	150	5.00	1.25	2.14	2.10	1.81394	0.64526
16	390	145	0.70	3.60	1.94	1.81	1.44024	0.58978
17	580	220	1.40	0.75	2.04	2.08	1.47050	0.70756
18	1100	400	2.50	0.40	1.97	2.07	1.54160	0.75696
19	200	425	1.80	0.20	1.83	2.03	0.72631	0.61461
20	650	310	1.90	3.00	1.96	1.84	1.18987	0.52285
21	280	330	0.90	2.40	2.09	1.99	0.74902	0.52820
22	600	300	0.30	0.45	1.98	2.09	1.35085	0.79805
23	720	190	3.50	2.60	2.11	1.99	1.63216	0.54418
24	225	495	0.80	2.10	2.03	1.94	0.57300	0.48519
25	750	390	0.65	0.40	2.02	2.13	1.30519	0.76752
26	600	600	1.25	0.75	1.89	1.93	0.93187	0.63901
27	330	240	0.30	0.08	1.78	2.10	1.18878	0.80137
28	875	160	0.70	0.06	1.76	2.19	2.27886	0.89415
29	1250	300	0.40	5.00	2.17	1.97	1.76635	0.62060
30	880	275	0.60	15.00	2.21	1.83	1.38503	0.45143
31	400	210	1.75	0.50	1.90	1.98	1.29553	0.72030
32	800	450	0.40	20.00	2.24	1.76	0.95347	0.45202
33	260	325	1.70	1.90	1.85	1.79	0.73450	0.51161
34	900	350	0.80	8.00	2.15	1.89	1.25556	0.48095
35	850	225	2.40	9.00	2.07	1.79	1.49872	0.39927
36	350	155	1.25	2.00	2.10	2.02	1.27767	0.59548
37	375	185	3.00	10.00	2.15	1.83	0.87565	0.36040
38	375	185	0.75	0.65	2.03	2.07	1.31661	0.73397
39	375	375	0.35	0.15	1.93	2.17	1.00493	0.74984
40	375	375	1.50	2.50	2.14	2.04	0.76000	0.49883
41	750	185	0.40	2.50	2.07	1.96	1.80950	0.69823
42	750	185	1.50	0.15	1.88	2.12	1.92167	0.84562
43	750	375	0.75	10.00	2.12	1.81	1.05797	0.45853
44	750	375	3.00	0.60	1.91	1.95	1.30850	0.69908
45	325	300	2.25	0.05	1.76	2.24	1.06733	0.76576

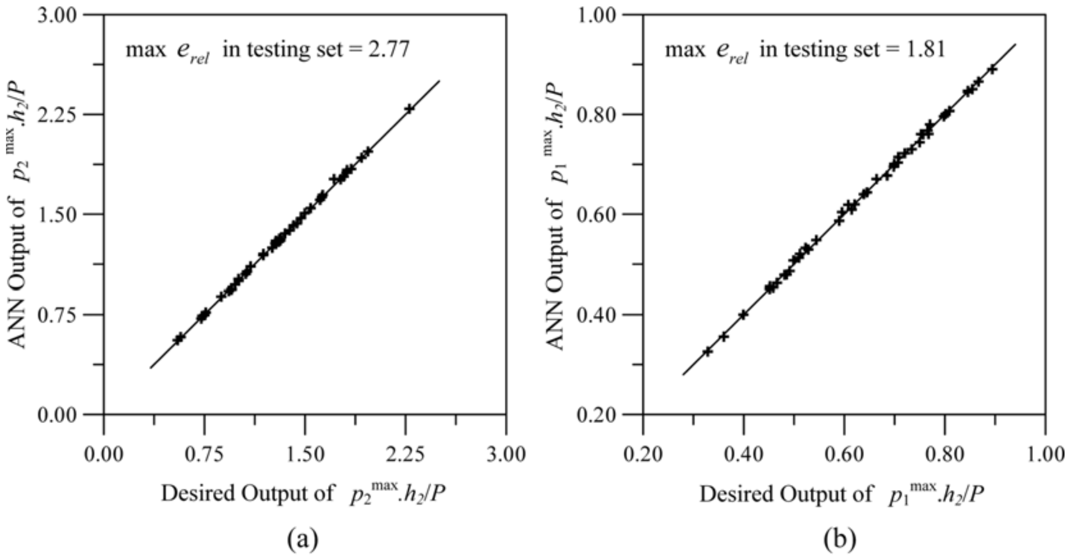

Fig. 4 Comparison of $p_2^{max} \cdot h_2/P$ and $p_1^{max} \cdot h_2/P$ obtained from ANN prediction and theoretical solution

$p_1^{max} \cdot h_2/P$. Each point stands for a testing pattern output. The nearer the points gather around the diagonal, the better are the learning results.

Once trained well, ANN can quickly predict the corresponding output(s) for any given inputs. In the following, the trained ANN is used to predict the effect of some factors on the dimensionless parameters related to the maximum contact pressures; $p_2^{max} \cdot h_2/P$ and $p_1^{max} \cdot h_2/P$, and the results are compared with theoretical solutions.

Fig. 5 shows the variation of the $p_2^{max} \cdot h_2/P$ and $p_1^{max} \cdot h_2/P$ with η = (200, 300, 450, 650, 900,

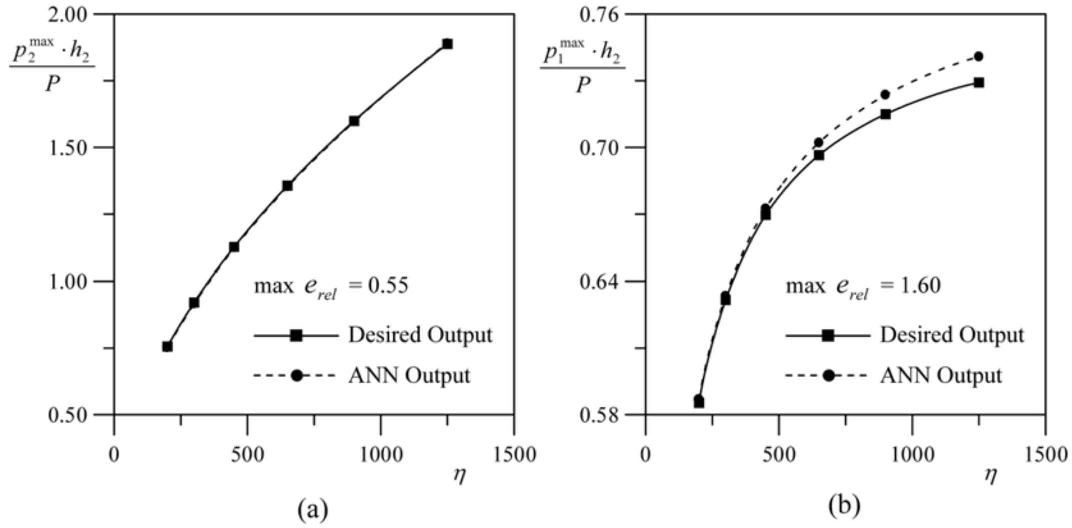

Fig. 5 Effect of η on $p_2^{max} \cdot h_2/P$ and $p_1^{max} \cdot h_2/P$ obtained from ANN prediction and theoretical solution

1250) for $R/h_2 = 300$, $h_2/h_1 = 1.25$, $\mu_2/\mu_1 = 0.80$, $\kappa_2 = 1.93$ and $\kappa_1 = 1.97$. It is seen that as η increases, while the other input values are fixed, $p_2^{\max} \cdot h_2/P$ and $p_1^{\max} \cdot h_2/P$ increase. Pattern input values are selected different from those in the train and test sets. Maximum relative errors are 0.55% and 1.60%, respectively.

Fig. 6 demonstrates the variation of $p_2^{\max} \cdot h_2/P$ and $p_1^{\max} \cdot h_2/P$ with $R/h_2 = (100, 150, 225, 325, 450, 625)$ for $\eta = 425$, $h_2/h_1 = 0.80$, $\mu_2/\mu_1 = 2.00$, $\kappa_2 = 2.14$ and $\kappa_1 = 2.06$. It is seen that as R/h_2 increases, while the other input values are fixed, $p_2^{\max} \cdot h_2/P$ and $p_1^{\max} \cdot h_2/P$ decrease. None of the pattern input values are selected same as those in the train and test sets. Maximum relative errors are 1.16% and 0.68%, respectively.

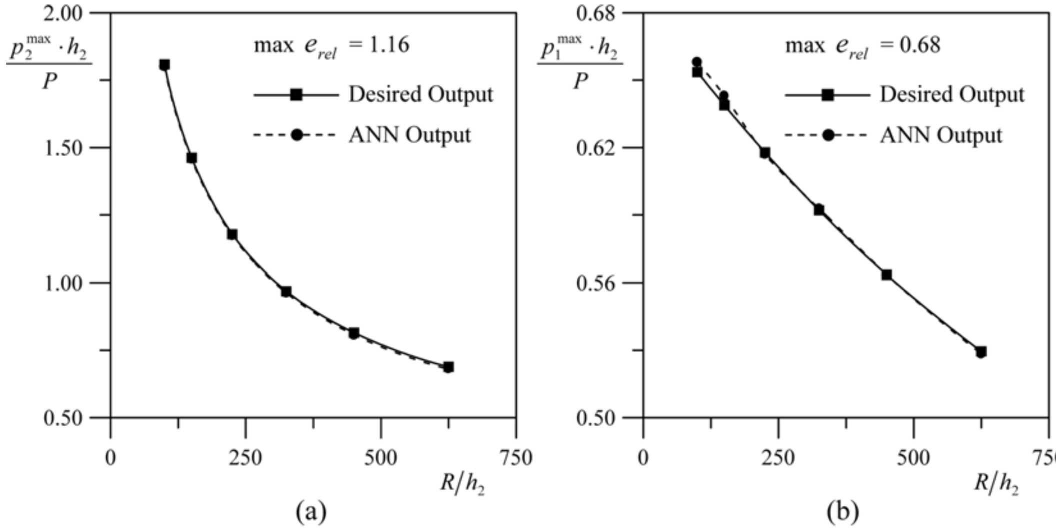

Fig. 6 Effect of R/h_2 on $p_2^{\max} \cdot h_2/P$ and $p_1^{\max} \cdot h_2/P$ obtained from ANN prediction and theoretical solution

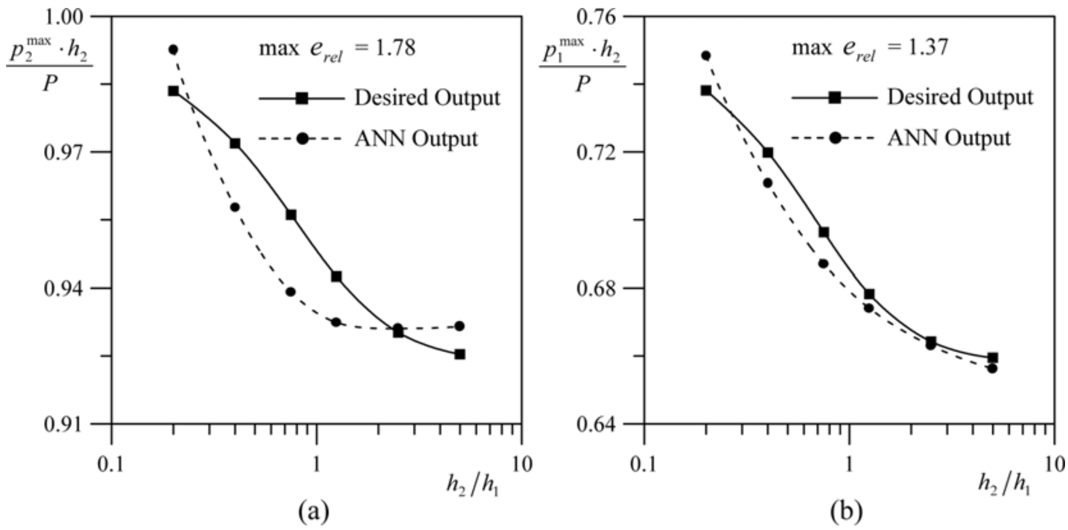

Fig. 7 Effect of h_2/h_1 on $p_2^{\max} \cdot h_2/P$ and $p_1^{\max} \cdot h_2/P$ obtained from ANN prediction and theoretical solution

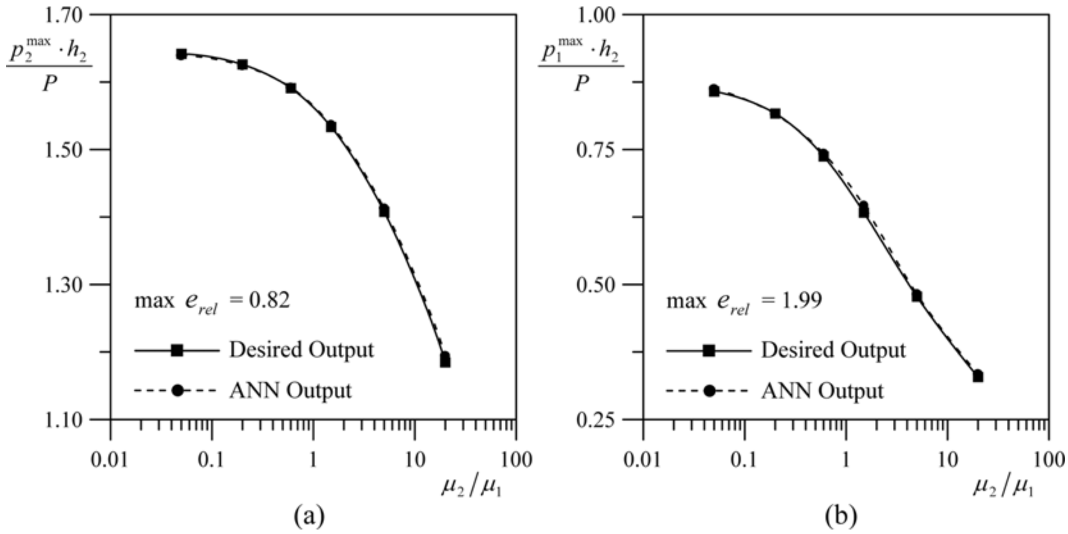

Fig. 8 Effect of μ_2/μ_1 on $p_2^{\max} \cdot h_2/P$ and $p_1^{\max} \cdot h_2/P$ obtained from ANN prediction and theoretical solution

Variation of $p_2^{\max} \cdot h_2/P$ and $p_1^{\max} \cdot h_2/P$ with $h_2/h_1 = (0.20,\ 0.40,\ 0.75,\ 1.25,\ 2.50,\ 5.00)$ for $\eta = 325$, $R/h_2 = 325$, $\mu_2/\mu_1 = 0.40$, $\kappa_2 = 2.05$ and $\kappa_1 = 2.15$ is given in Fig. 7. It is seen that as h_2/h_1 increases, while the other input values are fixed, $p_2^{\max} \cdot h_2/P$ and $p_1^{\max} \cdot h_2/P$ decrease. Pattern input values are also selected different from those in the train and test sets. Maximum relative errors are 1.78% and 1.37%, respectively.

Variation of $p_2^{\max} \cdot h_2/P$ and $p_1^{\max} \cdot h_2/P$ with $\mu_2/\mu_1 = (0.05,\ 0.20,\ 0.60,\ 1.50,\ 5.00,\ 20.00)$ for $\eta = 600$, $R/h_2 = 200$, $h_2/h_1 = 1.50$, $\kappa_2 = 2.00$ and $\kappa_1 = 2.00$ is given in Fig. 8. It is seen that as μ_2/μ_1 increases, while the other input values are fixed, $p_2^{\max} \cdot h_2/P$ and $p_1^{\max} \cdot h_2/P$ decrease. None of the pattern input values are also selected same as those in the train and test sets. Maximum relative errors are 0.82% and 1.99%, respectively.

5. Conclusions

In this paper, a tree layered artificial neural network with backpropagation algorithm has been developed. Reliable predictions have been produced for the dimensionless parameters related to the maximum contact pressures between the rigid stamp and the upper elastic strip, and between the two elastic strips. The patterns are obtained from elasticity solution. It is seen that, number of processing elements in the hidden layer, initial weight values and learning rate have considerable effects on the training. It was found that the artificial neural networks reduce the overall computation time required when compared with existing theoretical analysis methods.

As a result of using the artificial neural network in the analysis of the relationship between the dimensionless parameters related to the maximum contact pressures and the dimensionless quantity given in Eq. (7d), the ratio of radius of rigid stamp to upper elastic strip height, the ratio of upper and lower elastic strip heights, the ratio of upper and lower elastic strip shear modulus, the elastic constants of the upper and lower strips, following conclusions can be made:

- When η increases, $p_2^{\max} \cdot h_2/P$ and $p_1^{\max} \cdot h_2/P$ increase.
- $p_2^{\max} \cdot h_2/P$ and $p_1^{\max} \cdot h_2/P$ decrease, when R/h_2 increases.
- If h_2/h_1 increases, $p_2^{\max} \cdot h_2/P$ and $p_1^{\max} \cdot h_2/P$ decrease.
- $p_2^{\max} \cdot h_2/P$ and $p_1^{\max} \cdot h_2/P$ decrease, if μ_2/μ_1 increases.

It is shown that the artificial neural network predictions agree well with that of theoretical solutions in Figs. 4, 5, 6 and 8. However, good agreement is not observed in Fig. 7. Although the errors are not big in Fig. 7, agreement isn't like the same in Figs. 5, 6 and 8. It mustn't be forgotten that ANNs predict only with its capacity based on the training set patterns, so that; any predictions, except the testing set patterns used in this paper, doesn't guarantied to be agreed well and to have low relative errors. Consequently, based on the figures above, application of artificial neural networks to contact problems can be practical especially for the time consuming problems which require interpolation and iteration in theoretical solution. Artificial neural networks may be applied other contact problems successfully.

References

Arslan, A. and Ince, R. (1996), "The neural network approximation to the size effect in fracture of cementitious materials", *Eng. Fract. Mech.*, **54**(2), 249-261.

Chandrashekhara, K., Okafor, C.A. and Jiang, Y.P. (1998), "Estimation of contact force on composite plates using impact-included strain and neural networks", *Composites Part B*, **29B**, 363-370.

Comez, I., Birinci, A. and Erdol, R. (2004), "Double receding contact problem for a rigid stamp and two elastic layers", *European J. Mech. - A/Solids*, **23**(2), 301-309.

Erdogan, F. and Gupta, G. (1972), "On the numerical solutions of singular integral equations", *Quarterly J. Appl. Math.*, **29**, 525-534.

Fausett, L. (1994), *Fundamentals of Neural Networks*, Prentice-Hall, New Jersey.

Hajela, P. and Berke, L. (1991), "Neurobiological computational models in structural analysis and design", *Comput. Struct.*, **41**(4), 657-667.

Hegazy, T., Tully, S. and Marzouk, H. (1998), "A neural network approach for predicting the structural behavior of concrete slabs", *Canadian J. Civil Eng.*, **25**, 668-677.

Ghaboussi, J., Garrett, J.H. and Wu, X. (1991), "Knowledge based modeling of material behavior with neural networks", *J. Eng. Mech.*, **117**(1), 132-153.

Guranatram, D.J. and Gero, J.S. (1994), "Effect of representation on the performance of neural networks in structural engineering applications", *Microcomputers in Civil Engineering*, **9**(2), 97-108.

Masri, S.F., Nakamura, M., Chassiakos, A.G. and Caughey, T.K. (1996), "Neural network approach to detection of changes in structural parameters", *J. Eng. Mech.*, **122**(4), 350-360.

Ni, H.-G. and Wang, J.-Z. (2000), "Prediction of compressive strength of concrete by neural networks", *Cement and Concrete Research*, **30**, 1245-1250.

Ozsahin, T.S., Birinci, A. and Cakiroglu, A.O. (2004), "Prediction of contact lengths between an elastic layer and two elastic circular punches with neural networks", *Struct. Eng. Mech., An Int. J.,* **18**(4), 441-459.

Rumelhart, D.E., Hinton, G.E. and Williams, R.J. (1986), "Learning internal representations by error propagation", in Rumelhart, D.E. and McClelland, J.L., eds., *Parallel Distributed Processing*, MIT Press, Cambridge, 318-362.

Sanad, A. and Saka, M.P. (2001), "Prediction of ultimate shear strength of reinforced-concrete deep beams using neural networks", *J. Struct. Eng.*, **127**(7), 818-828.

Seibi, A. and Al-Alawi, S.M. (1997), "Prediction of fracture toughness using artificial neural networks (ANNs)", *Eng. Fract. Mech.*, **56**(3), 311-319.

Theocaris, P.S. and Panagiotopoulos, P.D. (1995), "Generalised hardening plasticity approximated via anisotropic

elasticity: A neural network approach", *Comput. Meth. Appl. Mech. Eng.*, **125**, 123-139.
Vanluchene, R.D. and Sun, R. (1990), "Neural networks in structural engineering", *Microcomputers in Civil Engineering*, **5**(3), 207-215.
Xiang, Y. and Tso, S.K. (2002), "Detection and classification of flaws in concrete structure using bispectra and neural networks", *NDT&E International*, **35**, 19-27.
Zurada, J.M. (1992), *Introduction to Artificial Neural Systems*, West Publishing Company, New York.